Nonreciprocal Spin Current Generation in Surface-Oxidized Copper Films

Genki Okano,[1] Mamoru Matsuo,[2,3] Yuichi Ohnuma,[2,3] Sadamichi Maekawa,[3,2] and Yukio Nozaki[1,4,*]
[1]Department of Physics, Keio University, Yokohama 223-8522, Japan
[2]Kavli Institute for Theoretical Sciences, University of Chinese Academy of Sciences, Beijing 100190, China
[3]RIKEN Center for Emergent Matter Science (CEMS), Wako 351-0198, Japan
[4]Center for Spintronics Research Network, Keio University, Yokohama 223-8522, Japan

(Received 8 August 2018; published 29 May 2019)

We experimentally demonstrate the nonreciprocal generation of spin current (J_s) in a surface-oxidized copper film. The efficiency of conversion is at least 320 times larger than the inverse conversion. This nonreciprocity is due to a novel type of J_s generation, which relies on the transfer of angular momentum from the velocity field of free electrons. A gradient in the electrical mobility in the film produces vorticity in the in-plane drift velocity of the free electrons. The inverse process can hardly occur when J_s is collinear with the gradient in the electrical mobility.

DOI: 10.1103/PhysRevLett.122.217701

A spin current (J_s) is a flow of spin angular momentum without an accompanying electric charge, and it has been widely used to control various spintronics devices [1,2]. Because J_s carries no electrical charge, there is no accompanying Joule heating, which greatly reduces the energy consumption in electronic devices. Moreover, J_s can exert a torque on magnetization more efficiently than can the Oersted field. Thus, J_s is essential for ultralow-power-consumption spintronic devices. The spin-Hall [3,4] and Rashba-Edelstein [5–7] effects (i.e., SHE and REE, respectively) have been widely investigated for the mutual conversion between charge current (J_c) and J_s. The SHE is based on bulk spin-orbit interactions (SOIs), while an interfacial SOI plays an important role in the REE. We note that the inverse effects to the SHE [8–12] and REE [13–15]—that is, the conversion from J_s to J_c—have been successfully demonstrated, and the efficiencies of the direct and inverse conversions have been reported to differ only by a small factor [11,16–19]. Mutual conversion has also been demonstrated in some topological surfaces [20–24], and the mutual conversion efficiencies differ by about an order of magnitude in Bi_2Se_3 systems [25,26]. Thus, the realization of mutual conversion between J_c and J_s suggests that the SOI-related phenomenon is always reciprocal.

In the present work, we demonstrate the nonreciprocal generation of a direct current (dc) J_s by applying a dc J_c to a surface-oxidized NiFe/Cu bilayer. The mutual conversion efficiency differs by at least a factor of 320, which suggests that J_s is generated in this system by a different mechanism than the SOI. Alternating current (ac) J_s generation via SOI in surface-oxidized Cu has been reported by An *et al.* [27]. However, the reciprocal SOI cannot fully explain our nonreciprocal phenomena. Namely, another charge-to-spin conversion mechanism is required in addition to the SOI in order to understand the nonreciprocal conversion between J_c and J_s. The nonreciprocal J_s generation can be attributed quantitatively to the angular momentum of the charge current—i.e., to the vorticity of the free-electron flow—which appears in a surface-oxidized Cu film in which the electrical mobility has a strong gradient with depth. Recently, similar J_s generations using the vorticity have been observed in liquid Hg [28,29] and surface-acoustic-wave (SAW) injected Cu film [30,31]. We have found that the amplitude of the J_s generated in a surface-oxidized Cu film is quantitatively consistent with the value obtained analytically by accounting for the distribution of the electrical mobility in a surface-oxidize Cu film. Conversely, when a J_s is applied parallel to the direction along which the electrical mobility varies, there is no vorticity owing to an electron flow caused by an external field. Consequently, the inverse conversion cannot occur.

In the present work, we have examined the reciprocity of J_s generation for the four bilayers NiFe(5)/Pt(10), Pt(10)/NiFe(5), NiFe(5)/Cu*(10), and Cu(10)/NiFe(5). Here, Cu* denotes surface-oxidized Cu, and all film thicknesses (given in parentheses above) are in nanometers. From the transmission electron microscopy of NiFe/Cu*, we confirmed that the oxidization was stopped approximately at 6 nm from the surface [32]. Namely, 4-nm-thick Cu remains nonoxidized in Cu*. All bilayers were patterned in the shapes of Hall bars, each with a nominal length $l = 20\ \mu$m and width of $w = 8\ \mu$m. We deposited a coplanar waveguide (CPW) consisting of Ti(5)/Au(100) on each of the bilayer samples, with an insulating SiO_2(70) layer deposited between the bilayer and the CPW for electrical insulation. To oxidize the top surface of the Cu film, we exposed the NiFe/Cu bilayer to air at room temperature for 40 h before depositing the SiO_2. In this

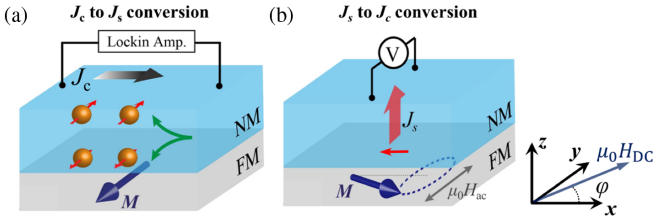

FIG. 1. (a) The experimental setup for the $J_c \Rightarrow J_s$ conversion study. We measured the first- and second-harmonic components of the longitudinal electrical resistance ($R_{xx}^{1\omega}$ and $R_{xx}^{2\omega}$) using the lock-in technique. (b) The experimental setup for the $J_s \Rightarrow J_c$ conversion experiment. By applying microwaves, we excited a ferromagnetic resonance (FMR) in the NiFe layer. A dc J_s is subsequently injected into the adjacent Pt or Cu* via the SP effect. If the Pt or Cu* possesses a large SOI, a voltage due to the inverse SHE occurs in the y direction.

work, we have examined the mutual conversions of the two bilayer samples, i.e., $J_c \Rightarrow J_s$ and $J_s \Rightarrow J_c$. Figure 1(a) shows a schematic illustration of the experimental setup we used to measure $J_c \Rightarrow J_s$ conversion. To characterize the magnetic and electrical properties of the bilayers, we performed second-harmonic measurements of both the longitudinal resistance $R_{xx}^{2\omega}$ and the transverse resistance $R_{xy}^{2\omega}$ as functions of the in-plane magnetic field, while applying an alternating current at the frequency $\omega/2\pi =$ 137 Hz to the bilayer. We applied external magnetic fields in the range from -300 to $+300$ mT at an in-plane angle φ from the x axis. The quantity $R_{xx}^{2\omega}$ contains resistance that arises from spin accumulation at the interface of each bilayer. The conversion efficiencies from J_c to J_s for Pt, Cu*, and Cu, $\theta_{J_c \Rightarrow J_s}^{\mathrm{Pt}}$, $\theta_{J_c \Rightarrow J_s}^{\mathrm{Cu}^*}$, and $\theta_{J_c \Rightarrow J_s}^{\mathrm{Cu}}$, respectively, can be evaluated from $R_{xx}^{2\omega}$, as we explain later. Figure 1(b) shows the schematic experimental setup for measuring the inverse conversion from J_s to J_c. We applied microwaves of power 20 dBm in the frequency range from 4 to 12 GHz to the CPW, and we applied an external magnetic field along the x axis. When the external magnetic field matched a ferromagnetic resonance (FMR) field of the NiFe, a FMR was excited in the NiFe layers, and the consequent J_s was injected into the adjacent nonmagnetic (NM) layer. If a sufficiently large SOI exists in the NM layer, the injected J_s is converted into J_c, which produces a Hall voltage across the bilayers. In this experiment, we evaluated $\theta_{J_s \Rightarrow J_c}^{\mathrm{Pt}}$, $\theta_{J_s \Rightarrow J_c}^{\mathrm{Cu}^*}$, and $\theta_{J_s \Rightarrow J_c}^{\mathrm{Cu}}$ from the Hall voltage. All measurements were carried out at room temperature.

We measured the unidirectional spin-Hall magnetoresistance (USMR) to evaluate $\theta_{J_c \Rightarrow J_s}^{\mathrm{Pt}}$, $\theta_{J_c \Rightarrow J_s}^{\mathrm{Cu}^*}$, and $\theta_{J_c \Rightarrow J_s}^{\mathrm{Cu}}$. The USMR is the magnetoresistance arising from the spin accumulation generated via the SHE at the interface of a bilayer consisting of a ferromagnetic and a nonmagnetic metallic thin film [44–48]. The USMR exhibits a nonlinear dependence of the electrical resistance on the current amplitude, which leads to unique unidirectional properties. Zhang *et al.* predicted theoretically that the nonlinear magnetoresistance can be attributed to spin-dependent interfacial scattering of electrons caused by the spin accumulation at the interface between the ferromagnetic and nonmagnetic films [46]. Owing to the USMR property that the electrical resistance exhibits a first-order variation with respect to the conversion efficiency $\theta_{J_c \Rightarrow J_s}$ [46], we can evaluate $\theta_{J_c \Rightarrow J_s}$ from the slope of the USMR as a function of the current. We also confirmed that a similar value of $\theta_{J_c \Rightarrow J_s}$ could be obtained from ST-FMR experiment [32].

Figures 2(a) and 2(b) show the values of $R_{xx}^{2\omega}$ measured for NiFe/Pt and NiFe/Cu*, respectively, while sweeping $\mu_0 H_y$ from -300 to $+300$ mT. In both cases, the absolute value of $R_{xx}^{2\omega}$ becomes constant when the magnetization saturates in the y direction, although the sign of the saturated value of $R_{xx}^{2\omega}$ depends on the magnetization direction. In the NiFe/Pt bilayer, rapid increases in $|R_{xx}^{2\omega}|$ appear when $|\mu_0 H_y|$ is smaller than 30 mT, which we attribute to the appearance of multidomain structure [44].

There are two possible reasons for this change in $R_{xx}^{2\omega}$: (1) the USMR and (2) the anomalous Nernst effect (ANE). Spin accumulation at the FM-NM interface leads to a change in $R_{xx}^{2\omega}$ due to the USMR, for which the amplitude depends linearly on the amount of J_s produced in the NM layer. When a dc J_c is applied along the x axis of the NiFe/Pt bilayer, a J_s is generated in the thickness direction (i.e., along the z axis) with its spin polarized along the y axis. In this case, the resistance of the NiFe/Pt varies with the magnetization direction of the NiFe: parallel or antiparallel to the injected spin. In consequence, a

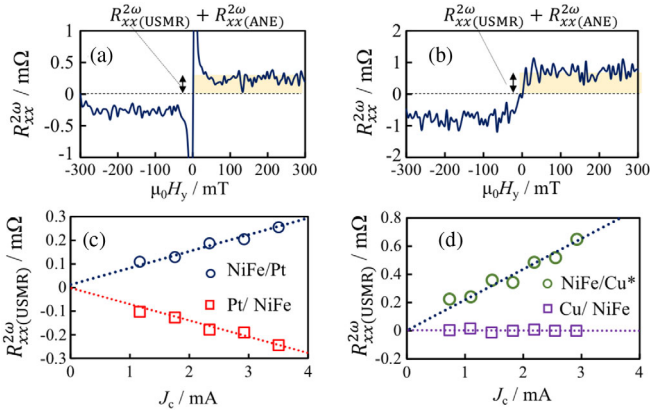

FIG. 2. $R_{xx}^{2\omega}$ for (a) the NiFe/Pt and (b) NiFe/Cu* bilayers. Here, $R_{xx}^{2\omega}$ denote the 2ω components of the longitudinal resistance. The vertical arrows in panels (a) and (b) represent the scale of USMR combined with ANE; see text for details. The J_c dependence of $R_{xx(\mathrm{USMR})}^{2\omega}$ for (c) Pt and (d) Cu bilayers, as measured at $\varphi = (\pi/2)$. Here, $R_{xx(\mathrm{USMR})}^{2\omega} = R_{xx}^{2\omega} - R_{xx(\mathrm{ANE})}^{2\omega}$. The slope of the J_c dependence of $R_{xx(\mathrm{USMR})}^{2\omega}$ gives $\theta_{J_c \Rightarrow J_s}^{\mathrm{Pt}}$ in (c) and $\theta_{J_c \Rightarrow J_s}^{\mathrm{Cu}^*}$ and $\theta_{J_c \Rightarrow J_s}^{\mathrm{Cu}}$ in (d).

second-harmonic component of the resistance appears. The ANE also leads to a change in the second-harmonic resistance ($R^{2\omega}_{xx(\mathrm{ANE})}$) [44,49]. If the electrical conductivity is widely distributed through the bilayer, a gradient of the Joule heating (∇T) appears along the z axis, and a consequent voltage drop due to the ANE is produced in the direction perpendicular to both the magnetization M and ∇T; consequently, $R^{2\omega}_{xx(\mathrm{ANE})}$ also has a $\sin\varphi$ dependence, which is the same as that of $R^{2\omega}_{xx(\mathrm{USMR})}$. The voltage drop due to the ANE can be evaluated separately by measuring the second-harmonic component of the transverse resistance ($R^{2\omega}_{xy}$) [42,49]. Taking account of the influence of the ANE on the second-harmonic component of the resistance, we obtain the following values of $R^{2\omega}_{xx(\mathrm{USMR})}$ when $\varphi = \pi/2$: $R^{2\omega}_{xx(\mathrm{USMR})} = 1.44R^{2\omega}_{xx}$ for NiFe/Pt and $R^{2\omega}_{xx(\mathrm{USMR})} = 0.81R^{2\omega}_{xx}$ for NiFe/Cu*.

To determine the magnitudes of $\theta^{\mathrm{Pt}}_{J_c\Rightarrow J_s}$ and $\theta^{\mathrm{Cu}^*}_{J_c\Rightarrow J_s}$ from these values of $R^{2\omega}_{xx(\mathrm{USMR})}$, we measured the J_c dependence of $R^{2\omega}_{xx(\mathrm{USMR})}$. The plots in Fig. 2(c) show $R^{2\omega}_{xx(\mathrm{USMR})}$ for the NiFe/Pt and Pt/NiFe bilayers, as a function of J_c. The spin accumulation at the interface depends linearly on J_c, because the J_s produced via SHE is proportional to J_c. In consequence, $R^{2\omega}_{xx(\mathrm{USMR})}$ increases linearly with J_c. Figure 2(d) shows the J_c dependence of $R^{2\omega}_{xx(\mathrm{USMR})}$ for the NiFe/Cu* and Cu/NiFe bilayers. The value of $R^{2\omega}_{xx(\mathrm{USMR})}$ for NiFe/Cu* increases linearly with J_c, while for Cu/NiFe $R^{2\omega}_{xx(\mathrm{USMR})}$ is negligibly small. The result clearly indicates that the Cu* can generate J_s.

We evaluated the magnitudes of $\theta^{\mathrm{Pt}}_{J_c\Rightarrow J_s}$, $\theta^{\mathrm{Cu}^*}_{J_c\Rightarrow J_s}$, and $\theta^{\mathrm{Cu}}_{J_c\Rightarrow J_s}$ from the $R^{2\omega}_{xx(\mathrm{USMR})}$. The conversion efficiencies can be evaluated from the slopes of Figs. 2(c) and 2(d) [32]. In this way, we finally obtain $\theta^{\mathrm{Pt}}_{J_c\Rightarrow J_s} \approx 0.064$, $\theta^{\mathrm{Cu}^*}_{J_c\Rightarrow J_s} \approx 0.032$, and $\theta^{\mathrm{Cu}}_{J_c\Rightarrow J_s} \approx 0.0035$. Note that $\theta^{\mathrm{Pt}}_{J_c\Rightarrow J_s}$ and $\theta^{\mathrm{Cu}^*}_{J_c\Rightarrow J_s}$ are the same order of magnitude. The relative amplitude of the conversion efficiency for Cu* is similar to that found in the previous study by An *et al.*, although they measured the spin-torque FMR (ST-FMR) at a frequency of a few GHz to obtain the ac rather than the dc J_s generation [27].

Next, we show experimental evidence that it is hard for the Cu* film to produce J_c from J_s. The inverse conversion from the dc J_s generated by the spin-pumping (SP) effect [50–53] to the dc J_c can be evaluated using the inverse SHE in the same NiFe/Cu* bilayer. Spin accumulates at the interface of the bilayer due to the excitation of a FMR in the NiFe film and J_s is subsequently injected into the adjacent Cu film. A dc voltage due to the inverse SHE is observed if the SOI of the Cu* film is sufficiently large. In this measurement, a dc J_s with spin polarization along the x axis was converted into J_c, producing a Hall voltage V_y along the y axis. The polarity of the voltage drop due to the inverse SHE is expected to be identical between Pt and Cu*,

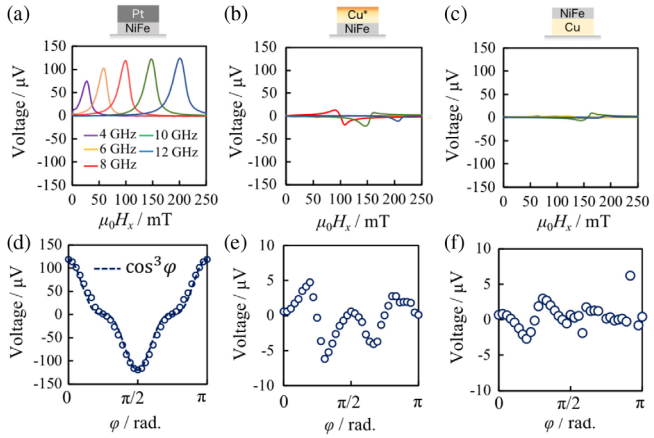

FIG. 3. Dependence of V_y on $\mu_0 H_x$ for (a) NiFe/Pt, (b) NiFe/Cu*, and (c) Cu/NiFe, as measured by applying microwaves. Clear Lorentz spectra are obtained at each frequency in (a), while (b),(c) show negligibly small Lorentz spectra. The φ dependence of the Lorentzian component of V_y in (d) NiFe/Pt, (e) NiFe/Cu*, and (f) Cu/NiFe bilayers at a frequency of 6 GHz.

because the conversion efficiencies from J_c to J_s measured using the USMR are positive for both Pt and Cu*. Note that in order to exclude scatter due to variations among the samples, we used identical samples to measure the USMR and the inverse SHE.

Figures 3(a)–3(c) show the dependence of V_y on $\mu_0 H_x$. We obtained spectra with amplitudes of only a few microvolts for (b) NiFe/Cu* and (c) Cu/NiFe, a much smaller magnitude than for (a) NiFe/Pt. Note that the spectrum of V_y includes both Lorentzian and anti-Lorentzian components, which are generally due to the inverse SHE and the magnetogalvanic effects, respectively. For NiFe/Pt, the Lorentzian peaks appeared clearly at each frequency. Figures 3(d)–3(f) show the φ dependences of the Lorentzian components of the V_y spectra measured at 6 GHz, where the rectification signal is minimized [32], for the NiFe/Pt, NiFe/Cu* and Cu/NiFe bilayers, respectively. The inverse SHE voltage is known to be proportional to $\cos^3\varphi$ [54]. Indeed, as indicated by the broken line in Fig. 3(d), the amplitude of the Lorentzian component in the V_y spectrum does exhibit a $\cos^3\varphi$ variation. Conversely, for NiFe/Cu* and Cu/NiFe, the amplitude of the Lorentzian component is negligibly small, and a frequency-dependent anti-Lorentzian component appears in the V_y spectra.

The relationship between $\theta_{J_s\Rightarrow J_c}$ and the converted inverse SHE voltage V_y is given by

$$V_y = w\rho\theta_{J_{s\Rightarrow J_c}}\lambda_{\mathrm{NM}}\tanh\left(\frac{d_{\mathrm{NM}}}{2\lambda_{\mathrm{NM}}}\right)\left(\frac{2e}{\hbar}\right)j_s^{\mathrm{NM}}, \qquad (1)$$

where w is the width and ρ is the electric resistivity of the bilayer, λ_{NM} is the spin diffusion length and d_{NM} is the thickness of the NM layers, $\hbar$ is Planck's constant, e is

the electron charge, and j_s^{NM} is the spin current density at the interfaces of each bilayer with NM = Pt, Cu* and Cu. The amplitude of j_s at the NiFe/Pt interface can be evaluated from V_y for NiFe/Pt, because it is known that the charge-to-spin conversion via SOI in Pt is reciprocal, i.e., $\theta^{\mathrm{Pt}}_{J_c\Rightarrow J_s} = \theta^{\mathrm{Pt}}_{J_s\Rightarrow J_c}$ [11]. It is noted that the amplitude of j_s is proportional to a real part of mixing conductance $g_r^{\uparrow\downarrow}$, which can be evaluated from a FMR linewidth [55,56]. From the FMR experiments [32], $g_r^{\uparrow\downarrow}$ for NiFe/Pt, NiFe/Cu*, and Cu/NiFe interfaces were evaluated as $2.02 \pm 0.28 \times 10^{19}$ m^{-2}, $0.26 \pm 0.07 \times 10^{19}$ m^{-2}, and $0.21 \pm 0.06 \times 10^{19}$ m^{-2}, respectively. We can, therefore, estimate $j_s^{\mathrm{Cu}^*}$ and j_s^{Cu} from the j_s^{Pt}. Finally, from V_y for NiFe/Cu* and Cu/NiFe, $\theta^{\mathrm{Cu}^*}_{J_s\Rightarrow J_c}$ and $\theta^{\mathrm{Cu}}_{J_s\Rightarrow J_c}$ can be evaluated at 0.0040 and 0.0039, respectively. Circles and squares in Fig. 4(a) are $\theta_{J_c\Rightarrow J_s}$ and $\theta_{J_s\Rightarrow J_c}$ values, respectively, evaluated for Cu* and Cu. As shown in Fig. 4(a), $\theta^{\mathrm{Cu}^*}_{J_c\Rightarrow J_s}$ is much larger than $\theta^{\mathrm{Cu}}_{J_c\Rightarrow J_s}$, although $\theta^{\mathrm{Cu}^*}_{J_s\Rightarrow J_c}$ and $\theta^{\mathrm{Cu}}_{J_s\Rightarrow J_c}$ are similar to the spin Hall angle reported for Cu film [56]. The result suggests that there is another nonreciprocal charge-to-spin conversion mechanism in addition to the SOI of Cu film. The nonreciprocity of the additional charge-to-spin conversion in Cu* defined by

$$\text{nonreciprocity} = \frac{\theta^{\mathrm{Cu}^*}_{J_c\Rightarrow J_s} - \theta^{\mathrm{Cu}}_{J_c\Rightarrow J_s}}{\theta^{\mathrm{Cu}^*}_{J_s\Rightarrow J_c} - \theta^{\mathrm{Cu}}_{J_s\Rightarrow J_c}} \tag{2}$$

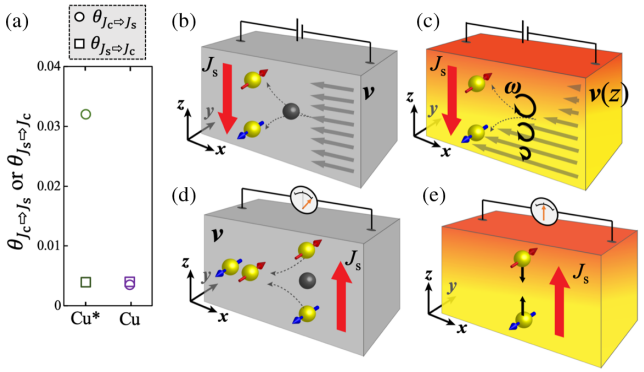

FIG. 4. (a) Direct and inverse charge-to-spin conversion efficiencies evaluated for NiFe/Cu* and Cu/NiFe. Schematic illustrations of the conversion from J_c to J_s in (b) Pt and (c) Cu*, and the inverse conversion from J_s to J_c in (d) Pt and (e) Cu*. The drift velocity of electrons is denoted as $\boldsymbol{v}$. The circular arrows in (c) represent the vorticity of electric current, $\boldsymbol{\omega}(z) = \nabla \times \boldsymbol{v}(z)$, produced in the surface-oxidized Cu film, which is caused by the gradient of the electrical mobility along the z axis. The dark shading in (c) and (e) represents the spatially varying oxidization of the Cu. The black sphere in (b) and (d) represents a scattering center, which produces spin-dependent scattering due to the SOI. In (e), J_s to J_c conversion does not occur because of the absence of vorticity.

is as large as 320 which cannot be explained by conventional charge-to-spin conversion theories based on SOI.

In this Letter, we have demonstrated dc J_s generation in surface-oxidized Cu by utilizing the USMR. An *et al.* have proposed that the J_s generation is attributable to the bulk SHE, because the Rashba coefficient obtained from their experiment is much larger than the highest values reported for metals [27]. Indeed, recent experimental results show that the SOI for Cu* is as large as that of Au and only about 4 times smaller than that for Pt [57]. However, the experimental results shown in Fig. 4(a) suggest that the J_s generated in the Cu* is not in accordance with the reciprocal SHE but requires a nonreciprocal mechanism. Moreover, we observed a nontrivial dependence of the USMR in NiFe/Cu* on an air exposure time which also supported that a novel mechanism of the nonreciprocal J_s generation existed in Cu* [32].

One possible mechanism for the nonreciprocity of the J_s generation is spin-vorticity coupling (SVC), which enables the conversion of a macroscopic angular momentum due to mechanical rotation into a microscopic spin angular momentum [29,30]. In particular, the mechanical rotation of a solid or fluid can be a source of spin accumulation. Indeed, J_s generation via SVC has been demonstrated using turbulence in liquid Hg [28] and using a Rayleigh-type surface acoustic wave in a Cu film [31]. In these systems, a vorticity field caused by a lattice motion acts on electron spins as an effective magnetic field [29,30], and leads to the J_c to J_s conversion along the gradient of the vorticity via SVC. Similarly, the vorticity gradient is induced in the Cu*, where a large gradient of the electrical mobility exists in the thickness direction. This is because the nonuniform mobility induces the spatially nonuniform distribution of the drift velocity of the conduction electrons as shown in Fig. 4(c). Thus, J_c is converted into J_s along the vorticity gradient via SVC. On the contrary, when J_s is injected into the oxidized Cu parallel to the gradient of the electrical conductance, the vorticity gradient is not generated because J_s is not accompanied by net drift velocity as shown in Fig. 4(e). Consequently, J_s cannot be converted into J_c.

We can estimate the magnitude of the J_s generated by angular-momentum transfer from the vorticity of the electron flow. Our model consists of two different materials with mobilities μ_{Cu} and $\mu_{\mathrm{Cu\text{-}O}}$ [32]. The transition region, where the electron mobility gradually varies over the length $2L$, is taken to be due to atomic interdiffusion between Cu and O atoms. We simply assume that the electrical mobility changes smoothly along the thickness direction as $\mu(z) \approx [(\mu_{\mathrm{Cu}} - \mu_{\mathrm{Cu\text{-}O}})/2][1 - \tanh(z/L)]$. Then, $\theta^{\mathrm{Cu}^*}_{J_c\Rightarrow J_s} - \theta^{\mathrm{Cu}}_{J_c\Rightarrow J_s}$ is given by

$$\theta^{\mathrm{Cu}^*}_{J_c\Rightarrow J_s} - \theta^{\mathrm{Cu}}_{J_c\Rightarrow J_s} \approx 0.051 \frac{l^2}{L^2}, \tag{3}$$

where l is the electron mean free path in Cu, and we assume that Cu-O($z > 4$ nm $+ 2L$) can be treated as an ideal insulator [32]. From the scanning transmission electron microscopy image of the cross section of the Cu* film, we identified $2L$ to be less than 6 nm [32]. Using $L = 3$ nm and $l = 4.6$ nm, evaluated from the relative electron conductivity of 10-nm-thick Cu*, we obtained $\theta^{\mathrm{Cu}^*}_{J_c \Rightarrow J_s} - \theta^{\mathrm{Cu}}_{J_c \Rightarrow J_s} \approx 0.12$, which is 4 times larger than the experiment. The overestimation is attributed to the fact that an electron mean free path at the transition region of oxide which plays an important role in J_s generation is shorter than the value evaluated from the averaged conductivity of Cu*.

In summary, we have demonstrated the nonreciprocal spin current generation as large as 320 in surface-oxidized Cu by using the USMR and SP. In the USMR experiment, surface-oxidized Cu generated finite J_s as large as that of Pt, while in the SP experiment, no spin to charge conversion was observed. One possible mechanism for the nonreciprocity is SVC, which originates in the vorticity gradient of electron flow in surface-oxidized Cu. From the viewpoint of applications, J_s generation via angular-momentum transfer from the vorticity of electron flow in an electrical-mobility-modulated film increases the freedom of material design for spintronics devices, because neither ferromagnets nor large SOI materials are necessary for a J_s generation.

The authors thank T. Horaguchi, K. Ando, and Y. Kageyama for valuable discussions. This work was supported by JSPS Core-to-Core Program and JSPS KAKENHI Grants No. JP17H05183 and No. JP18H03867. G. O. is supported by JSPS through a research fellowship for young scientists (No. JP18J20062).

*Corresponding author.
nozaki@phys.keio.ac.jp

[1] J. Åkerman, Science **308**, 508 (2005).
[2] T. Chen, R. K. Dumas, and A. Eklund, Proc. IEEE **104**, 1919 (2016).
[3] Y. K. Kato, R. C. Myers, A. C. Gossard, and D. D. Awschalom, Science **306**, 1910 (2004).
[4] J. Wunderlich, B. Kaestner, J. Sinova, and T. Jungwirth, Phys. Rev. Lett. **94**, 047204 (2005).
[5] V. M. Edelstein, Solid State Commun. **73**, 233 (1990).
[6] C. R. Ast, J. Henk, A. Ernst, L. Moreschini, M. C. Falub, D. Pacilé, P. Bruno, K. Kern, and M. Grioni, Phys. Rev. Lett. **98**, 186807 (2007).
[7] I. M. Miron, G. Gaudin, S. Auffret, B. Rodmacq, A. Schuhl, S. Pizzini, J. Vogel, and P. Gambardella, Nat. Mater. **9**, 230 (2010).
[8] E. Saitoh, M. Ueda, H. Miyajima, and G. Tatara, Appl. Phys. Lett. **88**, 182509 (2006).
[9] S. O. Valenzuela and M. Tinkham, Nature (London) **442**, 176 (2006).
[10] H. Zhao, E. J. Loren, H. M. van Driel, and A. L. Smirl, Phys. Rev. Lett. **96**, 246601 (2006).
[11] T. Kimura, Y. Otani, T. Sato, S. Takahashi, and S. Maekawa, Phys. Rev. Lett. **98**, 156601 (2007).
[12] S. Takahashi and S. Maekawa, J. Phys. Soc. Jpn. **77**, 031009 (2008).
[13] J.-C. Rojas Sánchez, L. Vila, G. Desfonds, S. Gambarelli, J. P. Attané, J. M. De Teresa, C. Magén, and A. Fert, Nat. Commun. **4**, 2944 (2013).
[14] J.-C. Rojas Sánchez, S. Oyarzún, Y. Fu, A. Marty, C. Vergnaud, S. Gambarelli, L. Vila, M. Jamet, Y. Ohtsubo, A. Taleb-Ibrahimi, P. Le Févre, F. Bertran, N. Reyren, J.-M. George, and A. Fert, Phys. Rev. Lett. **116**, 096602 (2016).
[15] E. Lesne, Yu Fu, S. Oyarzun, J.-C. Rojas-Sánchez, D. C. Vaz, H. Naganuma, G. Sicoli, J.-P. Attané, M. Jamet, E. Jacquet, J.-M. George, A. Barthélémy, H. Jaffrés, A. Fert, M. Bibes, and L. Vila, Nat. Mater. **15**, 1261 (2016).
[16] A. Hoffman, IEEE Trans. Magn. **49**, 5172 (2013).
[17] J. Sinova, S. O. Valenzuela, J. Wunderlich, C. H. Back, and T. Jungwirth, Rev. Mod. Phys. **87**, 1213 (2015).
[18] Y. Niimi and Y. Otani, Rep. Prog. Phys. **78**, 124501 (2015).
[19] Y. Ando and M. Shiraishi, J. Phys. Soc. Jpn. **86**, 011001 (2017).
[20] C. H. Li, O. M. J. vant Erve, J. T. Robinson, Y. Liu, L. Li, and B. T. Jonker, Nat. Nanotechnol. **9**, 218 (2014).
[21] Y. Shiomi, K. Nomura, Y. Kajiwara, K. Eto, M. Novak, Kouji Segawa, Yoichi Ando, and E. Saitoh, Phys. Rev. Lett. **113**, 196601 (2014).
[22] A. R. Mellnik, J. S. Lee, A. Richardella, J. L. Grab, P. J. Mintun, M. H. Fischer, A. Vaezi, A. Manchon, E.-A. Kim, N. Samarth, and D. C. Ralph, Nature (London) **511**, 449 (2014).
[23] Y. Fan, P. Upadhyaya, X. Kou, M. Lang, S. Takei, Z. Wang, J. Tang, L. He, L.-T. Chang, M. Montazeri, G. Yu, W. Jiang, T. Nie, R. N. Schwartz, Y. Tserkovnyak, and K. L. Wang, Nat. Mater. **10**, 699 (2014).
[24] Y. Ando, T. Hamasaki, T. Kurokawa, K. Ichiba, F. Yang, M. Novak, S. Sasaki, K. Segawa, Y. Ando, and M. Shiraishi, Nano Lett. **14**, 6226 (2014).
[25] P. Deorani, J. Son, K. Banerjee, N. Koirala, M. Brahlek, S. Oh, and H. Yang, Phys. Rev. B **90**, 094403 (2014).
[26] Y. Wang, P. Deorani, K. Banerjee, N. Koirala, M. Brahlek, S. Oh, and H. Yang, Phys. Rev. Lett. **114**, 257202 (2015).
[27] H. An, Y. Kageyama, Y. Kanno, N. Enishi, and K. Ando, Nat. Commun. **7**, 13069 (2016).
[28] R. Takahashi, M. Matsuo, M. Ono, K. Harii, H. Chudo, S. Okayasu, J. Ieda, S. Takahashi, S. Maekawa, and E. Saitoh, Nat. Phys. **12**, 52 (2016).
[29] M. Matsuo, Y. Ohnuma, and S. Maekawa, Phys. Rev. B **96**, 020401(R) (2017).
[30] M. Matsuo, J. Ieda, K. Harii, E. Saitoh, and S. Maekawa, Phys. Rev. B **87**, 180402(R) (2013).
[31] D. Kobayashi, T. Yoshikawa, M. Matsuo, R. Iguchi, S. Maekawa, E. Saitoh, and Y. Nozaki, Phys. Rev. Lett. **119**, 077202 (2017).
[32] See Supplemental Material at http://link.aps.org/supplemental/10.1103/PhysRevLett.122.217701 Sec. 1 for TEM image, Sec. 2 for ST-FMR experiment, which includes Refs. [33,34], Sec. 3 for removing ANE contribution, Sec. 4 for evaluating charge to spin conversion, Sec. 5 for evaluating the rectified signal contribution, Sec. 6 for FMR experiment by means of the VNA-FMR technique,

which includes Refs. [35,36], Sec. 7 for results of air-exposure time dependence of the USMR signal, which includes Refs. [37–40], Sec. 8 for the theoretical model of charge to spin conversion via spin vorticity coupling, which includes Refs. [41–43].

[33] L. Liu, T. Moriyama, D. C. Ralph, and R. A. Buhrman, Phys. Rev. Lett. **106**, 036601 (2011).

[34] W. Zhang, W. Han, X. Jiang, S.-H. Yang, and S. S. P. Parkin, Nat. Phys. **11**, 496 (2015).

[35] M. Harder, Z. X. Cao, Y. S. Gui, X. L. Fan, and C.-M. Hu, Phys. Rev. B **84**, 054423 (2011).

[36] M. Caminale, A. Ghosh, S. Auffret, U. Ebels, K. Ollefs, F. Wilhelm, A. Rogalev, and W. E. Bailey, Phys. Rev. B **94**, 014414 (2016).

[37] C. Gattinoni and A. Michaelides, Surf. Sci. Rep. **70**, 424 (2015).

[38] I. Zutić and A. Matos-Abiague, Nat. Phys. **12**, 24 (2016).

[39] D. Ciudad, Nat. Mater. **14**, 1188 (2015).

[40] J. Stajic, Science **350**, 924 (2015).

[41] D. Gall, J. Appl. Phys. **119**, 085101 (2016).

[42] A. F. Mayadas and M. Shatzkes, Phys. Rev. B **1**, 1382 (1970).

[43] J. S. Jin, J. S. Lee, and O. Kwon, Appl. Phys. Lett. **92**, 171910 (2008).

[44] C. O. Avci, K. Garello, A. Ghosh, M. Gabureac, S. F. Alvarado, and P. Gambardella, Nat. Phys. **11**, 570 (2015).

[45] C. O. Avci, K. Garello, J. Mendil, A. Ghosh, N. Blasakis, M. Gabureac, M. Trassin, M. Fiebig, and P. Gambardella, Appl. Phys. Lett. **107**, 192405 (2015).

[46] S. S. L. Zhang and G. Vignale, Phys. Rev. B **94**, 140411(R) (2016).

[47] C. O. Avci, M. Mann, A. J. Tan, P. Gambardella, and G. S. D. Beach, Appl. Phys. Lett. **110**, 203506 (2017).

[48] Y. Lv, J. Kally, D. Zhang, J. S. Lee, M. Jamali, N. Samarth, and J.-P. Wang, Nat. Commun. **9**, 111 (2018).

[49] C. O. Avci, K. Garello, M. Gabureac, A. Ghosh, A. Fuhrer, S. F. Alvarado, and P. Gambardella, Phys. Rev. B **90**, 224427 (2014).

[50] Y. Tserkovnyak, A. Brataas, and G. E. W. Bauer, Phys. Rev. Lett. **88**, 117601 (2002).

[51] S. Mizukami, Y. Ando, and T. Miyazaki, Phys. Rev. B **66**, 104413 (2002).

[52] Y. Tserkovnyak, A. Brataas, and G. E. W. Bauer, Phys. Rev. Lett. **88**, 117601 (2002).

[53] O. Mosendz, J. E. Pearson, F. Y. Fradin, G. E. W. Bauer, S. D. Bader, and A. Hoffmann, Phys. Rev. Lett. **104**, 046601 (2010).

[54] M. Harder, Y. Gui, and C.-M. Hu, Phys. Rep. **661**, 1 (2016).

[55] K. Ando, S. Takahashi, J. Ieda, Y. Kajiwara, H. Nakayama, T. Yoshino, K. Harii, Y. Fujikawa, M. Matsuo, S. Maekawa, and E. Saitoh, J. Appl. Phys. **109**, 103913 (2011).

[56] H. L. Wang, C. H. Du, Y. Pu, R. Adur, P. C. Hammel, and F. Y. Yang, Phys. Rev. Lett. **112**, 197201 (2014).

[57] R. Enoki, H. Gamou, M. Kohda, and J. Nitta, Appl. Phys. Express **11**, 033001 (2018).